BIBECHANA
ISSN 2091-0762 (Print), 2382-5340 (Online)
Journal homepage: http://nepjol.info/index.php/BIBECHANA
Publisher: Department of Physics, Mahendra Morang A.M. Campus, TU, Biratnagar, Nepal

Morphological analysis of Cu substituted Ni\Zn in Ni-Zn ferrites

D. Parajuli [1, 2*], K. Samatha[1]
[1]Department of Physics, Andhra University, Visakhapatnam, India
[2]Department of Physics, Tri-Chandra Multiple Campus, Tribhuvan University, Nepal
[*]Email: deepenparaj@gmail.com

Article Information:
Received: January 20, 2021
Accepted: May 6, 2021

Keywords:
Spinel
Ni-Zn ferrite
SEM-EDS
Critical concentration
Nucleation

ABSTRACT

Cu substituted Ni in $Ni_{0.5-x}Cu_xZn_{0.5}Fe_2O_4$ (x = 0, 0.05, 0.1, 0.15 and 0.2) samples and Cu substituted Zn in $Ni_{0.5}Zn_{0.5-x}Cu_xFe_2O_4$ (x = 0, 0.05, 0.1, 0.15 and 0.2) is synthesized using the sol-gel auto-combustion process. Recently, we have carried out their structural analysis using XRD and FTIR and found a cubic spinel structure. In this paper, we have studied their morphological and compositional structure with the help of a Scanning Electron Microscope (SEM) attached with an Energy Dispersive Spectrometer (EDS). The comparative study shows that the grain size of Cu substituted Ni is greater than Cu substituted Zn in Ni-Zn ferrite. These smaller grain-sized ferrites is preferred for many microstructural applications. Depending on the available magnetic field, sintering temperature, and atmosphere, they can have different nucleation, and hence their application mode is different. They can have a critical concentration that can tune their properties. The EDS attached with the SEM confirmed the proper composition of samples.

DOI: https://doi.org/10.3126/bibechana.v18i2.34383

1. Introduction

These spinel nanomaterials or ferrites are useful in the fields like microwave devices, ultra-high-density magnetic encoding, coating, etc. [1-3]. They have a crystallographic structure that can bring feasible change in their microstructure and electromagnetic characteristics. If the magnetic properties of those nanomaterials can be controlled then they can be exploited in advanced applications. Most of the spinel ferrite materials have an $M^{2+}Fe_2^{3+}O_4^{2-}$ type of structure, where, M is a Transitional Metal Cation. M is on the tetrahedral site and Fe on the octahedral site of the spinel. The study of the shape and material properties of different compositions of the Ni-Cu-Zn ferrite system is increasing these days [4-7]. Magnetic nanoparticles of Cu^{2+} added nickel-zinc magnetic oxides are commonly utilized in magnetic components for example rotary DY core, transformer, and magnetic inductive core. Similarly, the smaller grains coalesced together forming fine,

larger and non-uniform grains thereby decreasing intergranular porosity on the addition of Cu^{+2} contents. This property leads them applicable in high-frequency devices [8, 9]. The agglomeration indicates the strong interactions between the particles and grain growth during sintering [10] However, the cadmium substitution on decreases the grain size thereby decreasing dc electrical resistivity. Similarly, the magnetic saturation is decreased indicating the BB interaction i.e. interaction within the B site [11]. Recently, we have carried out the structural analysis using XRD and FTIR of Cu substituted $Ni_{0.5-x}Cu_xZn_{0.5}Fe_2O_4$ (x = 0, 0.05, 0.1, 0.15 and 0.2) samples and Cu substituted Zn in $Ni_{0.5}Zn_{0.5-x}Cu_xFe_2O_4$ (x = 0, 0.05, 0.1, 0.15 and 0.2) and found cubic spinel structure [12].

In the present study, it is planned to formulate nanoparticles of Cu substituted Ni and Cu substituted Zn in Ni-Zn ferrites containing iron oxide as their main components using the sol-gel auto combustion method. The structure and micro-texture of the material with appropriate heat treatment are analyzed.

2. Experimental Techniques and Materials

Copper Substituted Nickel-Zinc nanoparticles are prepared by the sol-gel auto-combustion method. 99.99% pure Nickel nitrate, Copper nitrate, Zinc nitrate, Iron nitrate, and citric acid monohydrate with the molecular formula (Ni $(NO_3)_2 \cdot 6H_2O$), Cu $(No_3)_3 \cdot H_2O$, (Zn $(NO_3)_2 \cdot 6H_2O$), (Fe $(NO_3)_3 \cdot 9H_2O$) and $(C_6H_8O_7.H_2O)$ respectively, as the starting materials. They are mixed in such a ratio that $Ni_{0.5-x}Cu_xZn_{0.5}Fe_2O_4$ (x = 0.0, 0.05, 0.1, 0.15 and 0.2) samples are prepared. The metal nitrates and citric acid were mixed in a molar ratio of 1:1 and were dissolved in the distilled water to get a clear solution. The solution was made neutral by adding liquid ammonia. The solution was then stirred in a magnetic stirrer maintained at 100°C for 4 hr, decanted, and dried at normal temperature for 40 hr. The flakes thus obtained were combusted and converted into a powder. The powder was sintered in a muffle furnace at 800 °C for 4 h at 5°/min. Similarly, $Ni_{0.5}Zn_{0.5-x}Cu_xFe_2O_4$ (x = 0, 0.05, 0.1, 0.15, and 0.2) are prepared with the same process in sintering temperature 900 °C in the air for 4 h and then followed by a natural cooling to room temperature. The surface morphology studies of all sintered pellets were characterized on a ZEISS scanning electron microscope with accelerating voltage 10 kV available in Analytical Research Laboratory, Andhra University, India. For making pallets, few drops of polyvinyl alcohol were mixed with the powder for shaping them into disc-like pallets after pressing them in a die under the hydraulic press of 5 tons. The pallets were then made as an electrode by sintering them in 800°C in a muffle furnace and polishing their flat sides with gold.

3. Results

A. Morphological Study

i. Morphological of Cu substituted Ni in Ni-Zn ferrite

The microstructural images like grain size, pores, inclusions, grain boundaries, particle size, homogeneity, defects, etc. can be obtained with the help of a Scanning Electron microscope. The smaller grain size with low porosity controls the unnecessary spin waves production which is essential for microwave devices. In the same way, the large grain size supports the mobility of the domain wall resulting in high permeability with low coercive value. Similarly, the eddy current losses are checked by the grain boundaries acting as current barriers. The SEM images (from Figure 1(a) to (e)) show that the nickel, copper, and zinc are not miscible and the average size of the grain is ranging from 0.2 to 0.4μm. The grains sizes are nearly equal to in the previous report [13].

ii. Morphological of Cu substituted Zn in Ni-Zn ferrite

The microstructural morphological study to investigate the grain size, uniformity, and shape of the Cu substituted Zn in Ni-Zn ferrite sintered at

900◦C was also done with the help of a ZEISS scanning electron microscope with accelerating voltage 10 kV as shown in Figure 2 (a-e). The figures show that the grain size is found to increase with copper content up to x=0.15 and then decreases for additional concentration similar to the previous reports [14, 15]. The turning point is called critical concentration. The electric and magnetic properties [16] of nanomaterials are significant for the uniform grain size and boundaries [17] measured by the linear intercept method. From the micrographs, the cupper content has improved the homogeneous spherical grain and low agglomeration similar to the result of Sundararajan et al. [15]. The grain size was found to be in the ranges from 130 to 246 nm with 130 nm for base composition, 183 nm for x=0.20, and the highest average grain size is 246 nm for x=0.15 similar to the previous results [18].

B. Compositional Study: Energy Dispersive Spectroscopy (EDS) Method

The elemental composition of the Ni-Zn ferrites was confirmed with the help of EDS and found the presence of O, Fe, Ni, and Zn as shown in Figure 3.

4. Discussion

Generally, the single grain is the composition of several crystals. The grain size depends on the sintering temperature and atmosphere [19]. They can be from very small colloidal particles, clay, silt, sand, gravel, cobbles to boulders. SEM study deals with the grain size of the materials which has a significant role in its electric, magnetic, mechanical properties, etc. Further, Ferrite grain size increase with temperature due to higher nucleation and copper content. As an example, ferrite grain size below 2mm transformed to cementite rather than pearlite as being small-sized austenite [20]. To get the size below 1mm, severe plastic deformation (SPD) process can be used which change the plate-shaped pearlite into a spherical cementite particle. This reduction in ferrite grain size from 5 to 1 μm increases the yield strength by 260 MPa. So, grain size reduction enhances the mechanical properties of the material. Further, the larger grain size is best for core loss, magnetic induction, and ac permeability in the weak magnetic field. For the smaller grain size, a larger field is needed for good performance [21]. Moreover, the size reduction produces the quantum confinement effect which we have studied in Metal Oxide Semiconductor especially ZnO and CdO The quantum confinement effects are significant in antibacterial activities. [22-23].

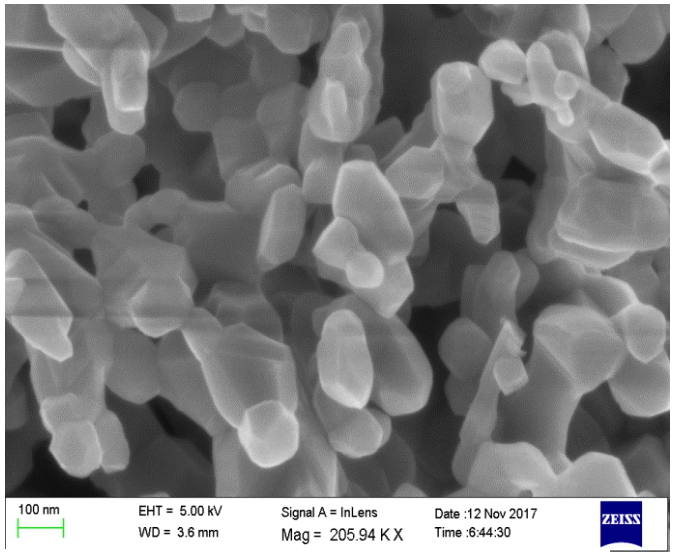

(a)

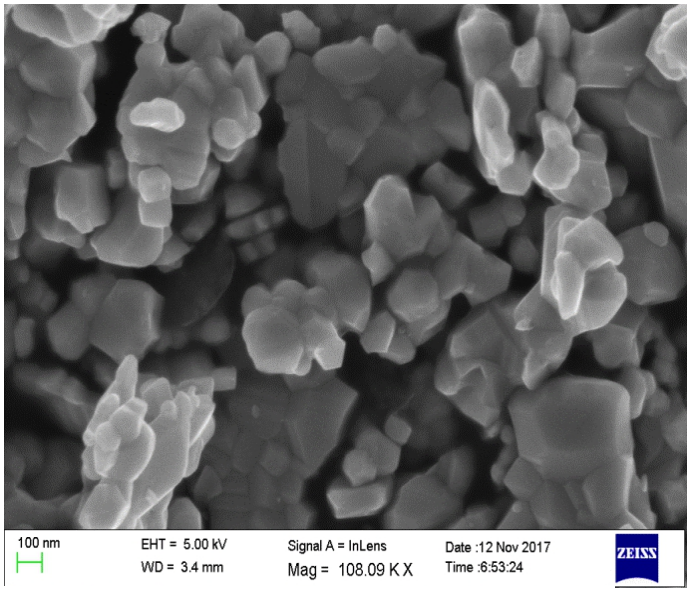

(b)

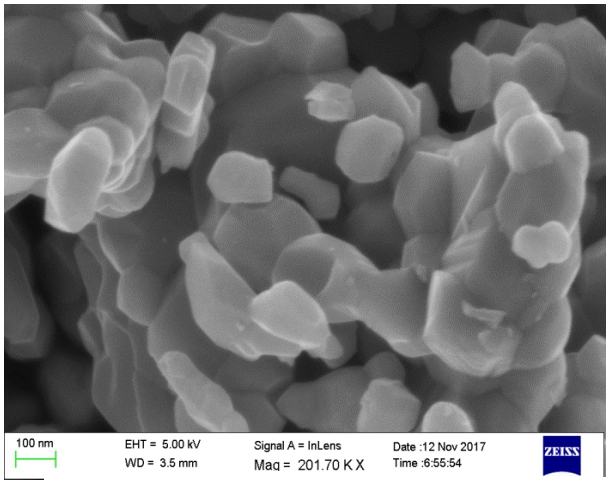

(c)

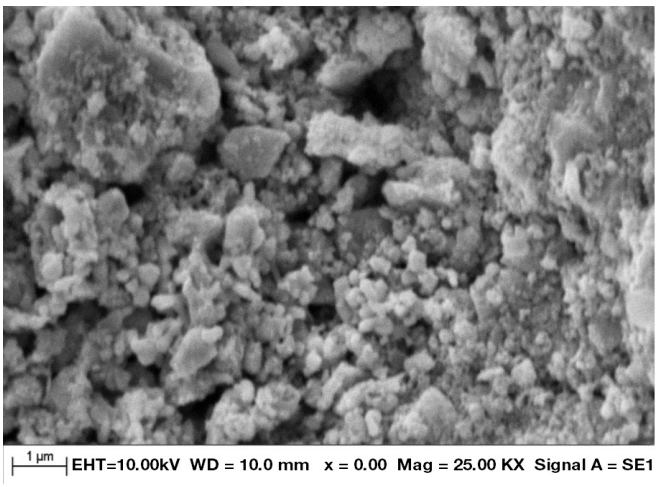

(a)

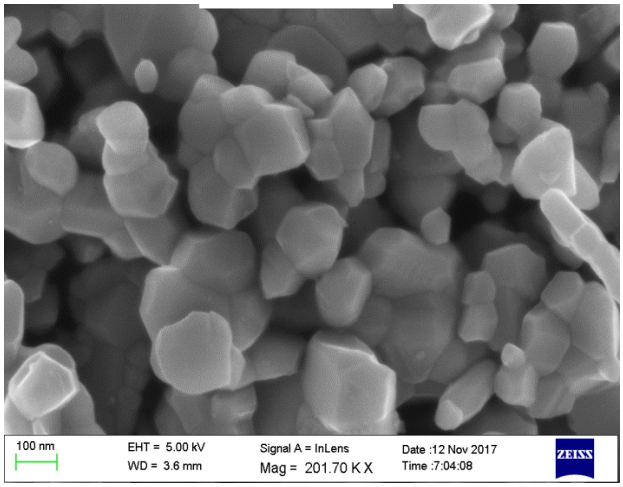

(d)

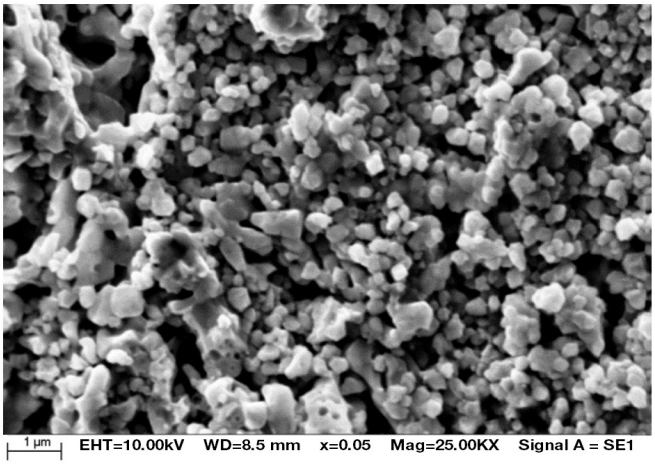

(b)

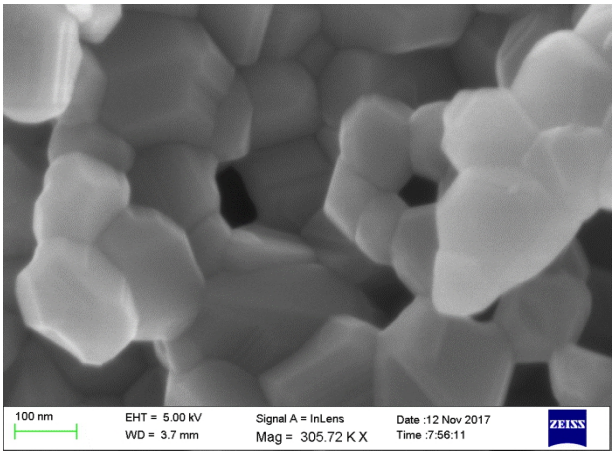

(e)

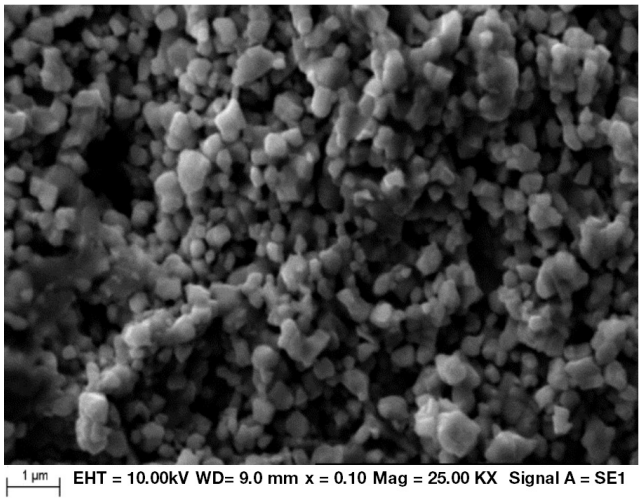

(c)

Fig. 1: (a) to (e): FESEM images for of $Ni_{0.5-x}Cu_xZn_{0.5}Fe_2O_4$ (x = 0.0, 0.05, 0.1, 0.15 and 0.2) ferrites

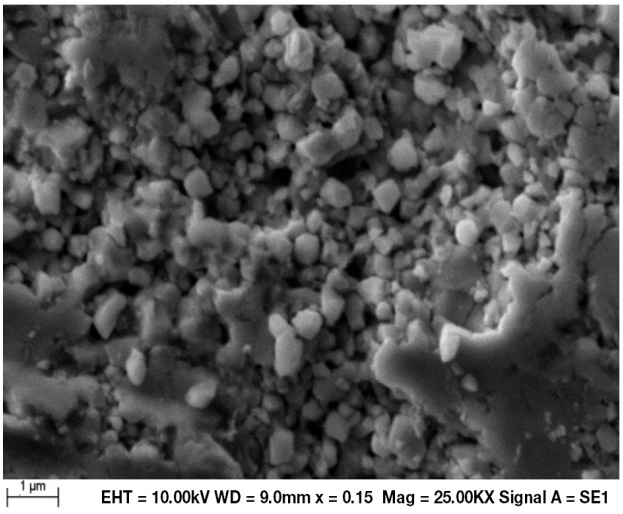

(d)

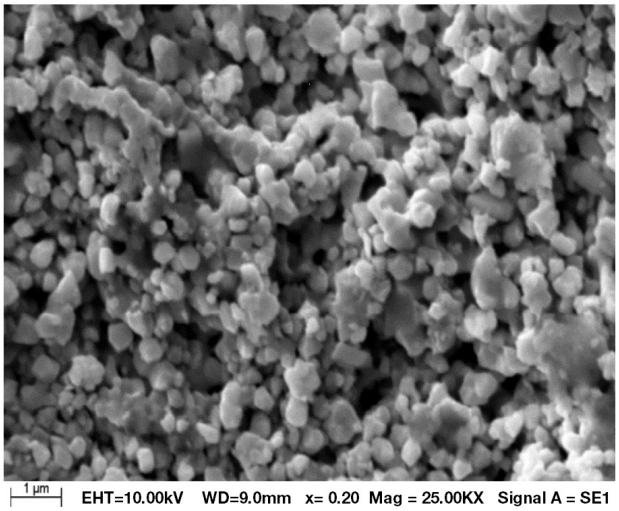

(e)

Fig. 2: (a-e): SEM micrographs of $Ni_{0.5}Zn_{0.5-x}Cu_xFe_2O_4$ (x = 0, 0.05, 0.1, 0.15 and 0.2) ferrites

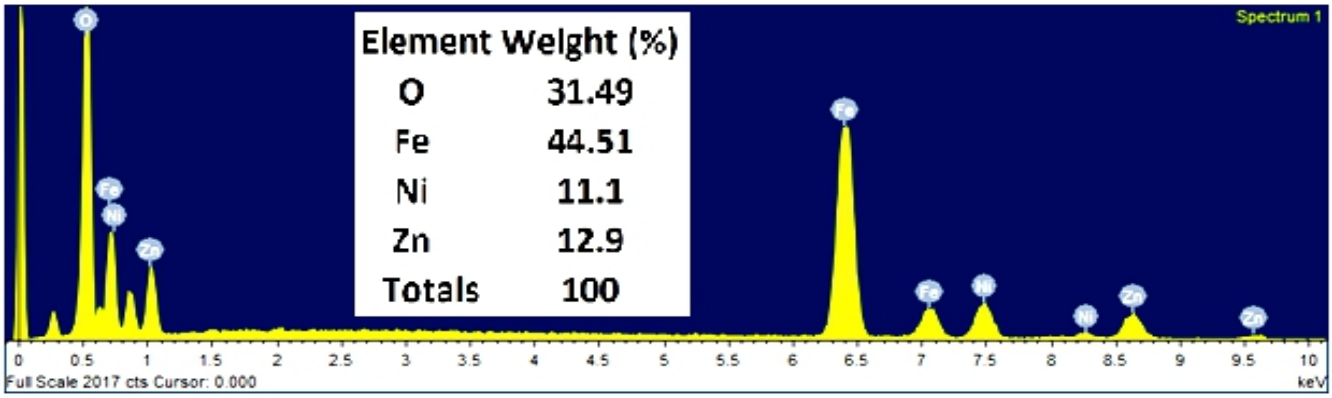

Fig. 3: EDS counts and elemental weight for $Ni_{0.5}Zn_{0.5}Fe_2O_4$ ferrite NPs

5. Conclusions

SEM micrograph of Cu substituted Ni in Ni-Zn ferrite reveals the microstructural growth along with heat action and the average size of the grain is ranging from 0.2 to 0.4µm or 200nm to 400nm. Cu substituted Zn in Ni-Zn ferrite makes it easy for sintering thereby improving grain formation, shape, and densification. SEM micrograph shows the increased grain size up to x=0.15 and then decreased for the gradual increase in the concentrations. The turning concentration x= 0.15 is the critical concentration beyond which the size is decreased and agglomeration occurs. The grain size was found to be in the ranges from 130 to 246 nm with 130 nm for base composition, 183 nm for x=0.20, and the highest average grain size is 246 nm for x=0.15. The comparative study shows that the grain size of Cu substituted Ni is greater than Cu substituted Zn in Ni-Zn ferrite. The smaller grain size is preferred for microstructural applications. The EDS attached with the SEM has given the proper composition of samples. The effect of grain size on the electric and magnetic properties will be discussed in the next paper.

References

[1] Shufang Yu, Guolin Wu, Xin Gu, Jingjing Wang, Yinong Wang, Hui Gao, Jianbiao Ma, Magnetic and pH-sensitive nanoparticles for antitumor drug delivery, Colloids Surf, 103 (2013) 15–22. https://doi.org/10.1016/j.colsurfb.2012.10.041

[2] Y. Tejabhiram, R. Pradeep, A. T. Helen, C. Gopalakrishnan, C. Ramasamy, Synthesis and magnetic properties of gadolinium substituted zinc ferrites, Mater. Res. Bull. 60 (2014) 778–82. https://doi.org/10.1016/j.matlet.2016.11.083

[3] D. K. Jha, M. Shameem, A. B. Patel, A. Kostka, P. Schneider, A. Erbe, P. Deb, Simple synthesis of superparamagnetic magnetite nanoparticles as highly efficient contrast agent, Mater. Lett. 95 (2013)186–189. https://doi.org/10.1016/j.matlet.2012.12.096

[4] S. Kenouche, J. Larionova, N. Bezzi, Y. Guari, N. Bertin, M. Zanca, L. Lartigue, M. Cieslak, C. Godin, C. Goze-Bac, NMR investigation of functionalized magnetic nanoparticles Fe3O4 as T1–T2 contrast agents, Powder Technol 225 (2014) 60–5. https://doi.org/10.1016/j.powtec.2013.07.038

[5] F. Geinguenaud, I. Souissi, R. Fagard, L. Motte, Y. Lalatonne, Electrostatic assembly of a DNA superparamagnetic nano-tool for simultaneous intracellular deliver y and in situ monitoring, Nanomed. Nanotechnol. Biol. Med. 8 (2012) 1106–15.
` https://doi.org/10.1016/j.nano.2011.12.010

[6] Ji Hyun Min, Mi-Kyung Woo, Ha Young Yoon, Jin Woo Jang, Jun Hua Wu, Chae-Seung Lim, Young Keun Kim, Isolation of DNA using magnetic nanoparticles coated with dimercaptosuccinic acid, Anal. Biochem. 447 (2014) 114–8. https://doi.org/10.1016/j.ab.2013.11.018

[7] A. Drmota, J. Koselj, M. Drofenik, A. Znidarsic, Electromagnetic wave absorption of polymeric nanocomposites based on ferrite with spinel and hexagonal crystal structure, J. Magn. Magn. Mater 324(2012)1225–9. https://doi.org/10.1016/j.jmmm.2011.11.015

[8] D. Parajuli, K. Samatha. Structural analysis of Cu substituted Ni/Zn in Ni-Zn Ferrite. BIBECHANA (2021) 18 (1) 128-133. https://doi.org/10.3126/bibechana.v18i1.29475.

[9] P Himakar, D. Parajuli, N Murali, V. Veeraiah, K. Samatha, Tulu Vegayehu Mammo, Mujasam Batoo Khalid, Hadi Muhammad, Raslan Emad, and Syed Farooq, Magnetic and DC Electrical Properties of Cu Doped Co-Zn Nanoferrites, Journal of Electronic Materials. https://doi.org/10.1007/s11664-021-08760-8 .

[10] K. Chandramouli, B. Suryanarayana, P.V.S.K Phanidhar Varma, V. Raghavendra, K. A. Emmanuel, P., Taddesse, N. Murali, Mammo, T. Wegayehu, D. Parajuli, Effect of Cr3+ substitution on dc electrical resistivity and magnetic properties of Cu0.7Co0.3Fe2-xCrxO4 ferrite nanoparticles prepared by sol-gel auto combustion method, Results in Physics (2021), https://doi.org/10.1016/j.rinp.2021.104117T

[11] Shaik Jesus Mercy· D. Parajuli N. Murali · A. Ramakrishna · Y. Ramakrishna · V. Veeraiah · K. Samatha, Microstructural, thermal, electrical and magnetic analysis of Mg2+ substituted Cobalt ferrite, Applied Physics A (2020) https://doi.org/10.1007/s00339-020-04048-6

[12] D. Parajuli, Vemuri Raghavendra, B. Suryanarayan, P. Anantha Rao, N. Murali, P.V.S. K. Phanidhar Varma, R. Giri Prasad, Y. Ramakrishna, K. Chandramouli, Taddesse Paulose. Cadmium substitution effect on structural, electrical, and magnetic properties of Ni-Zn nanoferrites. Results in Physics. Elsevier. https://doi.org/10.1016/j .rinp.2021.103947

[13] H. Jing, X. Wang, Y. Liu, A. Wang, Coppercobalt Bimetallic Oxides-doped Alumina Hollow Spheres: A Highly Efficient Catalyst for Epoxidation of Styrene, Chin. J. Catal. 36 (2) (2015) 244–51. https://doi.org/10.1016/S1872-2067(14)60221-7

[14] Z. Yue, J. Zhou, L. Li, H. Zhang, Z. Gui, Synthesis of nanocrystalline NiCuZn ferrite powders by sol-gel auto combustion method, J. Magn. Magn. Mater. 208 (2000) 55–60. https://doi.org/10.1016/S0955-2219(02)00082-1

[15] M. Sundararajan, Kennedy LJ, Photocatalytic removal of rhodamine B under irradiation of visible light using Co1− xCuxFe2O4 (0≤x≤0.5) nanoparticles, J. Environ. Chem. Eng. 5(4) (2017) 4075–4092. https://doi.org/10.1016/j.jece.2017.07.054

[16] J. Bera, P. K. Roy, Effect of grain size on electromagnetic properties of Ni0.7Zn0.3Fe2O4 ferrite, Physica B: Condensed Matter, Volume 363, Issues 1–4, (2005) 128-132. https://doi.org/10.1016/j.physb.2005.03.010.

[17] E.V. Gopalan, K.A. Malini, S. Saravanan, D.S. Kumar, Y. Yoshida, M.R. Anantharaman, Evidence for polaron conduction in nanostructured manganese ferrite, J. Phys. D Appl. Phys. 41 (2008)18500., https://doi.org/10.1088/0022-3727/41/18/185005

[18] D. Venkatesh and K. V. Ramesh. Structural and electrical properties of Cu-doped Ni–Zn nanocrystalline ferrites for MLCI applications, Modern Physics Letters B 31 (2017) 1750318, https://doi.org/10.1142/S0217984917503183.

[19] A. Hajalilou, Mansor Hashim, Halimah Mohamed Kamari, and Mohamad Taghi Masoudi, Effects of Milling Atmosphere and Increasing Sintering Temperature on the Magnetic Properties of Nanocrystalline Ni0.36Zn0.64Fe2O4, Journal of Nanomaterials, Hindawi Publishing Corporation. (2015). http://dx.doi.org/10.1155/2015/615739

[20] T. Tsuchida-Mayama, Nakano M., Uehara U., Sano M., Fujisawa N., Okada K., Sakai T. Mapping of the phosphorylation sites on the phototropic signal transducer, NPH3. Plant Sci. 174 (2008) 626–633. https://doi.org/10.1371/journal.pone.0001869

[21] M. Shiozaki, Kurosaki, Y. The effects of grain size on the magnetic properties of nonoriented electrical steel sheets, J. Materials Engineering 11, (1989) 37–43. https://doi.org/10.1007/BF02833752

[22] Umesh Reddy Gudla, B. Suryanarayana, Vemuri Raghavendra, D. Parajuli, N. Murali, Shouri Dominic, Y. Ramakrishna, and K. Chandramouli, Structural, optical and luminescence properties of pure, Fe-doped and glucose-capped CdO Semiconductor nanoparticles for their Antibacterial activity, J Mater Sci: Mater Electron(2021) 32:3920–3928. https://doi.org/10.1007/s10854-020-05135-3

[23] Umesh Reddy Gudlaa, B. Suryanarayanaa, Vemuri Raghavendrab, K.A. Emmanuelc, N. Muralia,, Paulos Taddessed, D. Parajulie, K. Chandra Babu Naidu, Y. Ramakrishnaa, K. Chandramouli, Optical and luminescence properties of pure, iron-doped, and glucose-capped ZnO nanoparticles. Contents lists available at ScienceDirect Results in Physics, Results in Physics, 19 (2020) 103508. https://doi.org/10.1016/j.rinp.2020.103508